Developmental Biology 320 (2008) 267–277

Contents lists available at ScienceDirect

Developmental Biology

journal homepage: www.elsevier.com/developmentalbiology

Lpp is involved in Wnt/PCP signaling and acts together with Scrib to mediate convergence and extension movements during zebrafish gastrulation

Hilke B.V.K. Vervenne [a], Koen R.M.O. Crombez [a,1], Kathleen Lambaerts [b], Lara Carvalho [c], Mathias Köppen [c], Carl-Philipp Heisenberg [c], Wim J.M. Van de Ven [a,*], Marleen M.R. Petit [a]

[a] Laboratory for Molecular Oncology, Department of Human Genetics, K.U. Leuven, Leuven, Belgium
[b] Laboratory of Glycobiology and Developmental Genetics, Department of Human Genetics, K.U. Leuven, Leuven, Belgium
[c] Max Planck Institute of Cell Biology and Genetics, Dresden, Germany

ARTICLE INFO

Article history:
Received for publication 7 September 2007
Revised 9 May 2008
Accepted 9 May 2008
Available online 20 May 2008

Keywords:
LPP
Scrib
Noncanonical Wnt signaling
Planar cell polarity
Convergence and extension
gastrulation

ABSTRACT

The zyxin-related LPP protein is localized at focal adhesions and cell–cell contacts and is involved in the regulation of smooth muscle cell migration. A known interaction partner of LPP in human is the tumor suppressor protein SCRIB. Knocking down *scrib* expression during zebrafish embryonic development results in defects of convergence and extension (C&E) movements, which occur during gastrulation and mediate elongation of the anterior–posterior body axis. Mediolateral cell polarization underlying C&E is regulated by a noncanonical Wnt signaling pathway constituting the vertebrate planar cell polarity (PCP) pathway. Here, we investigated the role of Lpp during early zebrafish development. We show that morpholino knockdown of *lpp* results in defects of C&E, phenocopying noncanonical Wnt signaling mutants. Time-lapse analysis associates the defective dorsal convergence movements with a reduced ability to migrate along straight paths. In addition, expression of Lpp is significantly reduced in Wnt11 morphants and in embryos overexpressing Wnt11 or a dominant-negative form of Rho kinase 2, which is a downstream effector of Wnt11, suggesting that Lpp expression is dependent on noncanonical Wnt signaling. Finally, we demonstrate that Lpp interacts with the PCP protein Scrib in zebrafish, and that Lpp and Scrib cooperate for the mediation of C&E.

Introduction

The *LPP* (*LIM domain containing preferred translocation partner in lipoma*) gene was previously identified as the most frequent translocation partner of *HMGA2* (*High Mobility Group A2*) in a subgroup of benign tumors of adipose tissue, i.e. lipomas with an aberration involving chromosome segment 12q15 harboring the *HMGA2* gene (Petit et al., 1996). In the years after its discovery, *LPP* was also shown to be rearranged in a number of other soft tissue tumors (Dahlen et al., 2003; Petit et al., 1998; Rogalla et al., 2000), as well as in a case of acute monoblastic leukemia (Daheron et al., 2001). In addition to its involvement in tumors, two independent laboratories identified LPP as a novel smooth muscle cell (SMC) marker (Gorenne et al., 2003; Nelander et al., 2003) and, in a recent follow-up study, LPP was shown to regulate SMC migration in vitro (Gorenne et al., 2006).

LPP is a member of the zyxin family of proteins, whose structure is characterized by the presence of multiple protein–protein interaction domains including C-terminally located LIM domains (Petit et al., 1996) (Fig. S1). LPP localizes in focal adhesions, which are sites of membrane attachment to the extracellular matrix, and in cell–cell contacts (Petit et al., 2003). It is able to interact with VASP (vasodilator-stimulated phosphoprotein) (Petit et al., 2000) and α-actinin (Li et al., 2003), both of which localize at cell adhesion sites. Of interest to note is that LPP is also able to shuttle to the nucleus, where it acts as a coactivator of the ETS-domain transcription factor PEA3 (Guo et al., 2006). PEA3 activates gene expression and is thought to play an important role in promoting tumor metastasis (Shepherd et al., 2001) but also in controlling neuronal development, including neuronal pathfinding (Livet et al., 2002). Recently, palladin, an actin-associated protein, was found to bind LPP and both proteins were shown to play an active role in the adhesion turnover of migrating SMCs (Jin et al., 2007).

Another known interaction partner of LPP in human is SCRIB (Petit et al., 2005b), a functional homologue of the *Drosophila* tumor suppressor Scribble (Bilder and Perrimon, 2000), which resides in cell–cell contacts, and is involved in the control of cell adhesion, cell shape and cell polarity. Scrib is implicated in the regulation of planar cell polarity (PCP) in vertebrates (Montcouquiol et al., 2003; Murdoch et al., 2003; Wada et al., 2005). The PCP pathway refers to a conserved signaling pathway that regulates the coordinated movements and polarity of cells or structures within the plane of an epithelium (For review, see Wang and Nathans, 2007). One of such movements is convergence and extension (C&E), a process that occurs during

* Corresponding author. Fax: +32 16 34 60 73.
E-mail address: wim.vandeven@med.kuleuven.be (W.J.M. Van de Ven).
[1] Current address: Bristol-Myers Squibb International Corporation — Research and Development, Parc de l'Alliance, Braine-l'Alleud, Belgium.

0012-1606/$ – see front matter © 2008 Elsevier Inc. All rights reserved.
doi:10.1016/j.ydbio.2008.05.529

gastrulation and results in elongation and narrowing of the embryonic body axis. These cell movements were shown to be impaired after knockdown of *scrib* in zebrafish (Wada et al., 2005).

Although the involvement of LPP in SMC migration in vitro and the different functions of its known interaction partners suggest a role for LPP in the regulation of cell migration in general, so far, nothing is known yet about its function in the complex context of an organism. Therefore, the aim of this study was to study the function of LPP using the zebrafish embryo as a model system. We investigated the role of the LPP orthologue in zebrafish (Lpp) in the regulation of C&E during early embryogenesis by applying the morpholino knockdown technique to suppress Lpp function. We also examined whether Lpp and Scrib interact in zebrafish as well, and, if they cooperate for the regulation of C&E.

Materials and methods

Maintenance and breeding of zebrafish

Wild-type AB zebrafish (*Danio rerio*) strains were maintained and bred according to standard protocols (Westerfield, 1995). Embryos were produced by natural mating and were collected and fixed at different stages based on standard morphological criteria (Kimmel et al., 1995).

RNA isolation and reverse transcriptase PCR (RT-PCR)

Total RNA was extracted from wild-type zebrafish embryos of different stages using Trizol reagent (Invitrogen, Carlsbad, California, USA) according to the manufacturer's instructions. cDNA was synthesized by reverse transcription of 5 μg total RNA, using random hexamer primers and Superscript II/III reverse transcriptase (Invitrogen, Carlsbad, California, USA). *lpp* mRNA was detected with primers Lpp-cds-up 5′-GTGACCAGCAAGGTCATGTG-3′ and Lpp-cds-rev 5′-TGTTGCAGTTTTTGCAGAGG-3′, amplifying the complete *lpp* coding sequence. As a control, expression of zebrafish *β-actin* mRNA was detected using primers bactin-up 5′-CACACCTTCTACAAT-3′ and bactin-rev 5′-ACTCCTGCTTGCTGA-3′. All primers used in this paper were purchased from Eurogentec (Seraing, Belgium).

Whole-mount in situ hybridization

Sense and antisense RNA probes against the 3′UTR of *lpp* were synthesized from DNA templates obtained by PCR in the following way: T7 or Sp6 promoter sequences (underlined) were appended to the 5′ end of the sense and antisense *lpp*-specific primers respectively (3′UTRzLpp-up 5′-GAAATATTTAGGTGACACTATAGGCTCACACGTG-TACATGCAG-3′ and 3′UTRzLpp-rev 5′-GAAATTAATACGACTCACTATAGGGCACCTTA-TATTGGTGGAAA-3′), and RT-PCR was performed using total cDNA from wild-type zebrafish embryos (0.5 hpf) as a template. In situ probes were synthesized from purified PCR products using a DIG RNA labeling kit (Roche). Antisense RNA probes against *hgg1* (Thisse et al., 1994), *dlx-3* (Akimenko et al., 1994) and *ntl* (Schulte-Merker et al., 1992) were synthesized from DNA templates (kind gift from W. Driever, University of Freiburg, Germany) using a DIG RNA labeling kit (Roche). Embryos were collected, fixed overnight in 4% paraformaldehyde (PFA) and washed 3 times in PBST (0.1% Tween-20 in PBS). Whole-mount in situ hybridizations were performed as described (Thisse and Thisse, 1998), except, anti-DIG incubation was performed for two h instead of overnight. After staining, embryos were fixed in 4% PFA. Stained embryos were mounted in 80% glycerol (in PBST) and analyzed using a Leica Fluo Combi stereomicroscope.

For *gsc*, *BMP4*, *chordin*, *myoD* and *papc*, generation of antisense RNA probes and in situ hybridizations were performed as described previously (Ulrich et al., 2005).

SDS-PAGE and Western blotting

Uninjected zebrafish embryos and embryos injected with Lpp-MM/ATG (5 ng) or Lpp-MO/ATG (5 ng) were collected at prim-5 stage. After removal of the yolk, 10 embryos of each condition were lysed by adding 20 μl of 2× SDS sample buffer (0.15 M Tris–HCl pH 6.7, 30% glycerol, 5% SDS, 4% β-mercapto-ethanol) and subsequent sonication. 20 μl of each lysate was heated at 95 °C for 5 min and was loaded on a 7.5% SDS-polyacrylamide gel. After size-separation, proteins were electrophoretically transferred to PROTEAN Nitrocellulose Membranes (Schleicher and Schuell, Keene, New Hampshire, USA). Amounts of protein loaded were verified by Ponceau S (Sigma-Aldrich, St. Louis, Missouri, USA) staining of the blot. Zebrafish Lpp was detected with a mouse monoclonal antibody (Clone 6.1, BD Biosciences, Transduction Laboratories) (dilution 1:2000), followed by incubation with horseradish peroxidase-conjugated rabbit anti-mouse IgG as secondary antibody (Dako, Glostrup, Denmark) (dilution 1:2000). Immunoreactive proteins were visualized using Western Lightning chemiluminescence reagent Plus (Perkin Elmer, Waltham, Massachusetts, USA), according to the supplier's instructions. The intensities of the signals were quantified using Kodak Digital Science (Kodak Imager with 1D Image Analysis Software, version 3.0).

Morpholino injections and rescue experiments

Two independent morpholinos against zebrafish *lpp* (Lpp-MO/ATG and Lpp-MO/3e3i), two mismatch control morpholinos (Lpp-MM/ATG and Lpp-MM/3e3i), and morpholinos against zebrafish *scrib* (Scrib-MO) (Wada et al., 2005), *trilobite* (Tri-MO) (Park and Moon, 2002) and zebrafish *wnt11* (Wnt11-MO) were used in the experiments. All morpholinos were dissolved at 40 μg/ml in 1x Danieau's solution (58 mM NaCl, 0.7 mM KCl, 0.4 mM $MgSO_4$, 0.6 mM $Ca(NO_3)_2$, 5.0 mM HEPES pH 7.3). RhodaminB-labeled dextrane was added to each sample as a control for injections. Injections were performed into the cell cytoplasm of one- or two-cell stage embryos, after which the embryos were incubated at 28.5 °C. After 6 h, unfertilized eggs, dead embryos and embryos that did not show homogenous fluorescence were removed. Embryos were analyzed using a Leica Fluo Combi stereomicroscope. Pictures were taken using a digital Leica DC300F camera connected to the stereomicroscope, and IM500 software.

Morpholino antisense oligomeres used are: LPP-MO/ATG 5′-ACCATCATTATGTCCG-CCCCACATG-3′; LPP-MM/ATG 5′-ACGATGATTATCTCCCCCCGACATG-3′; LPP-MO/3e3i 5′-GCTATCAATCTTACCCTCGTGTGTT-3′; LPP-MM/3e3i 5′-GCTATGAATGTTAG-CCCACGTCTGTT-3′; Scrib-MO 5′-CCACAGCGGGATCACTTCAGCATG-3′ (Wada et al., 2005); Wnt11-MO 5′-GTTCCTGTATTCTGTCATGTCGCTC-3′; Tri-MO 5′-GTACTGCGAC-TCGTTATCCATGTC-3′ (Park and Moon, 2002). Morpholinos directed against *lpp*, *scrib* and *trilobite* were purchased from GeneTools, LLC (Philomath, Oregon, USA). The Wnt11-MO was purchased from Open Biosystems (Huntsville, Alabama, USA).

For the rescue experiments, full-length wild-type zebrafish *lpp* cDNA (obtained by RT-PCR with primers Lpp1-up 5′-TCAACTCCAGAAACATGTGG-3′ and Lpp2-down 5′-TTCAGAGGTCAGTCGTGGCC-3′) was subcloned into the pBCM vector (kind gift from Dr. C. Esguerra, K.U. Leuven, Leuven, Belgium). pBCM is a modified version of the pbUT2 plasmid (Krieg and Melton, 1984) with additional modifications introduced by C. Esguerra and M. Haardt (unpublished). Capped mRNA was synthesized using the T3 promoter and the mMessage mMachine kit (Ambion, Austin, Texas, USA). Different amounts of wild-type synthetic *lpp* mRNA varying from 5 pg to 50 pg were titrated by co-injection with Lpp-MO/3e3i and by injection alone to reach an optimal level that could best rescue *lpp* morphants. The optimal dose of *lpp* mRNA (7.5 pg) was then used to rescue *lpp* morphants by co-injection with Lpp-MO/3e3i (5 ng) at the one- to two-cell stage.

RNA injections

Capped sense RNA encoding dnRok2 (kind gift from Prof. Dr. L. Solnica-Krezel, Vanderbilt University, Nashville, Tennessee, USA) and Wnt11 (kind gift from Prof. Dr. J Topczewski, Northwestern University Feinberg School of Medicine, Chicago, USA) were synthesized from linearized DNA templates using the Sp6 RNA polymerase (mMessage mMachine system; Ambion, Austin, Texas, USA). *dnRok2* transcripts were stabilized by adding a poly(A) tail (Poly(A) Tailing Kit; Ambion, Austin, Texas, USA). RNA injections were performed as described for the morpholinos.

Time-lapse imaging and image analysis

Dechorionated wild-type and Lpp-MO/ATG (5 ng) injected embryos were mounted dorsal side up in 1% low melting point agarose (Invitrogen) in an imaging chamber consisting of a glass ring on a glass slide. Paraxial mesodermal cells in tailbud stage embryos were photographed at 20x magnification with Nomarski optics using a Zeiss Axioplan2 imaging microscope and QImaging camera. Images were collected at 2 min intervals. Time-lapse recordings proceeded for 2 h at room temperature. The centers for individual cells were determined and their (x, y) coordinates recorded over time using ImageJ software. Cell migration paths, total speeds and net dorsal speeds were calculated using Microsoft Excel.

Comparison between migration speeds in wild-type and Lpp-MO/ATG injected embryos was analyzed using unpaired 2-tailed Student's t test ($p<0.05$ was considered significant) and standard error of the mean (Table S1).

Quantitative RT-PCR

Embryos injected with Wnt11-MO, *wnt11* RNA or *dnRok2* RNA were selected based on the presence of C&E defects. Total RNA extraction and cDNA synthesis was performed as described above for RT-PCR. Quantitative RT-PCR was performed using qPCR Master Mix for SYBR Green I detection and fluorescein as internal standard (Eurogentec, Seraing, Belgium) using the MyIQ system (Bio-Rad, Hercules, California, USA), in accordance with the manufacturer's guidelines. The relative amount of gene expression was calculated using the comparative C_t method ($2^{-\Delta\Delta Ct}$). *18 s rRNA* was used as a reference gene to correct for sample quality (Van Raay et al., 2007).

Primers used were: QRTLpp-up 5′-GGAGTATTTCGGTCGGTGTTCA-3′ and QRTLpp-rev 5′-CCCTCGCCAACCACATTCT-3′; QRT18s-up 5′-TGGTATCGGTCAGCATATTTTGA-3′ and QRT18s-rev 5′-AGCGCTGCCTTCTCTATGATG-3′. Primers were designed using Primer Express software (Applied Biosystems, Foster City, California, USA).

Comparisons between *lpp* expression levels in injected and uninjected embryos from four independent experiments were analyzed using paired 2-tailed Student's t test ($p<0.05$ was considered significant) and standard error of the mean.

In vitro transcription/translation and GST pull-down assay

All in vitro translation reactions were carried out using the TNT T7 Quick Coupled Transcription/Translation System (Promega, Madison, Wisconsin, USA)

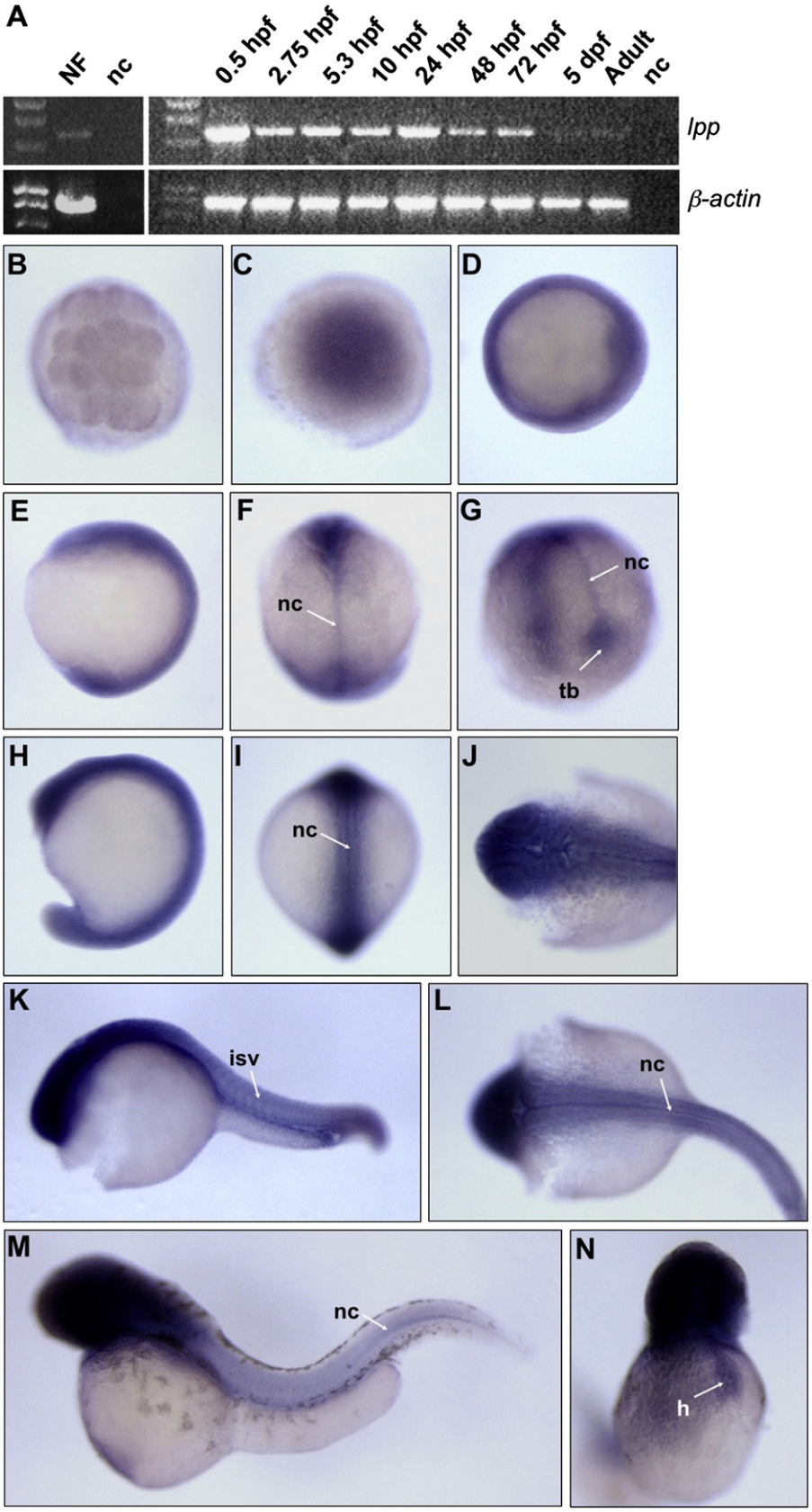

Fig. 1. Expression of *lpp* during zebrafish development. (A) Expression of *lpp* and *β-actin* mRNA as determined by RT-PCR at different stages of zebrafish development and in non-fertilized eggs (NF). nc, negative control. (B–N) Whole-mount in situ hybridization analyses for zebrafish *lpp* expression at different stages of embryonic development using an RNA probe against the 3′UTR of *lpp*. (B) 16-cell stage, animal pole view. (C) dome stage, animal pole view. (D) shield stage, animal pole view, dorsal to the right. (E) tailbud stage, lateral view, dorsal to the right. (F) tailbud stage, dorsal view, anterior on top. (G) tailbud stage, vegetal pole view. (H) 14-somite stage, lateral view, dorsal to the right. (I) 14-somite stage, dorsal view. (J) Prim-5 stage, head region, dorsal view. (K) Prim-5 stage, lateral view. (L) Prim-5 stage, dorsal view. (M) Long-pec stage, lateral view. (N) Long-pec stage, frontal view. *Abbreviations:* nc, notochord; tb, tailbud; isv, intersomitic vessels; h, heart.

following the manufacturer's instructions. For GST pull-down assays, bacterial expression constructs were made using pGEX-5X vectors (Amersham Biosciences, Piscataway, New Jersey, USA) directing the synthesis of glutathione S-transferase (GST) fusion proteins containing wild-type or mutated zebrafish Lpp. These fusion proteins were purified according to the manufacturer's instructions and purification was verified by SDS-PAGE. GST fusion proteins or GST alone, bound to glutathione-agarose beads, were incubated with an in vitro synthesized [^{35}S]methionine/cysteine-labeled portion of wild-type zebrafish Scrib protein, encompassing all four of the PDZ domains (AA 700–1517), in $NENT_{100}$ buffer (100 mM NaCl, 20 mM Tris–HCl pH 7.6, 1 mM EDTA, 0.1% NP-40, protease inhibitors). This mixture was tumbled overnight at 4 °C. Subsequently, the beads were washed 5 times in 500 µl $NENT_{100}$ buffer, resuspended in 30 µl SDS-PAGE sample buffer, and incubated at 95 °C for 5 min. Proteins were separated by SDS-PAGE and interacting Scrib was detected by autoradiography.

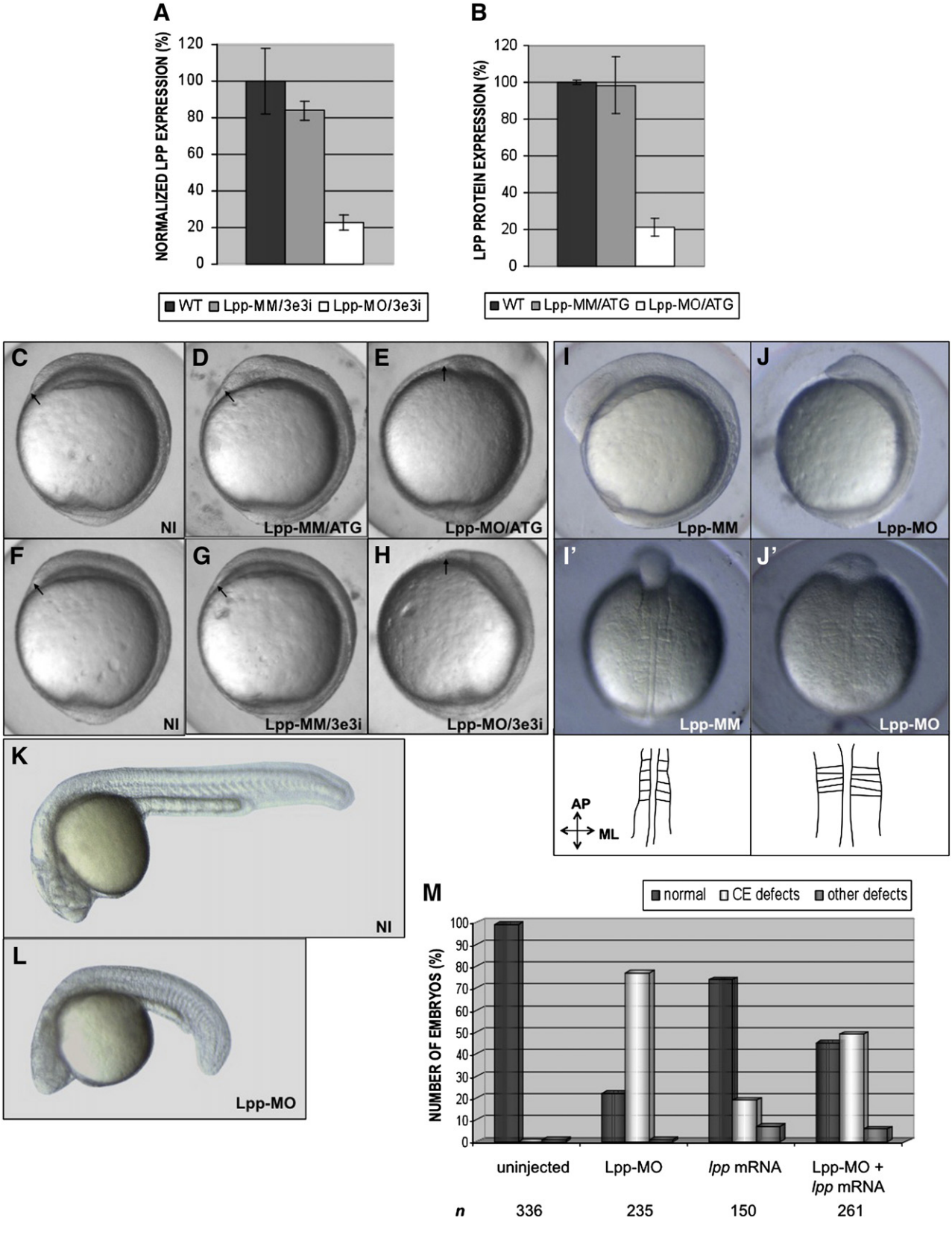

Results

Expression of lpp during zebrafish development

The zebrafish model was used to examine the function of LPP during vertebrate development. We performed a BLAST search in the NCBI zebrafish database with the amino acid sequence of human LPP to find an orthologue in zebrafish (Lpp). We found a predicted Lpp protein, encoded by the zebrafish *lpp* cDNA clone (GenBank accession no. BC050503), showing high sequence identity with human LPP in all of the formerly characterized functional domains, such as the LIM domains, the nuclear export signal (NES) and the binding sites for VASP, α-actinin and SCRIB (Fig. S2).

To understand the potential roles of Lpp during zebrafish development, its spatial and temporal expression pattern was examined. Therefore, we determined *lpp* expression at different stages of zebrafish development by reverse transcriptase PCR (RT-PCR), using primers that amplify the complete coding region of *lpp* (Fig. 1A). Expression of *lpp* was observed at all stages examined from 0.5 h post-fertilization (hpf) until adulthood (i.e. 3 months of age), although expression levels at stages from 4 days post-fertilization and later on were significantly lower (Fig. 1A and data not shown). As can be seen in Fig. 1A, *lpp* was also expressed in non-fertilized eggs, which indicates the presence of maternal transcripts. Whole-mount in situ hybridization analyses using an antisense RNA probe against the 3′UTR region of *lpp*, showed ubiquitous expression of *lpp* in all stages examined from 16-cell until shield stage (Figs. 1B–D). At tailbud stage *lpp* expression appeared to be enriched at the dorsal midline, in the tailbud and in the head region (Figs. 1F, G) and at 14-somite stage in the notochord (Fig. 1I). At prim-5 stage, *lpp* expression became intense in the head region (Figs. 1J–K), and was enriched in the intersomitic vessels (Fig. 1K) and notochord (Fig. 1L). At 2 days post fertilization, lpp expression was restricted to the head region, the notochord and the heart (Figs. 1M, N).

Morpholino-mediated knockdown of lpp expression interferes with zebrafish gastrulation

The function of Lpp in zebrafish was assessed by injection of morpholino antisense oligomeres at the one- to two-cell stage, which induces specific knockdown of Lpp protein expression. We used two independent morpholinos: a splice-block morpholino directed against the exon–intron boundary of the first coding exon (Lpp-MO/3e3i) and a translation-block morpholino targeting the translation start site (Lpp-MO/ATG) (Fig. S3). For each of the morpholinos, a mismatch control morpholino (Lpp-MM/3e3i and Lpp-MM/ATG respectively) was generated which contains 5 mismatches and cannot bind the *lpp* (pre-)mRNA properly. Efficiency of the splice-block morpholino was validated by quantitative RT-PCR. Injection of Lpp-MO/3e3i but not Lpp-MM/3e3i resulted in an 80% reduction of mature *lpp* mRNA levels at tailbud stage, as compared to the wild-type control (Fig. 2A). Efficiency of the translation-block MO was tested by Western blot, showing a robust reduction of Lpp protein band intensity after injection of Lpp-MO/ATG but not after injection of Lpp-MM/ATG at prim-5 stage, as compared to the wild-type control (Fig. 2B).

At the end of gastrulation, wild-type embryos have elongated anterior–posterior (AP) and narrow mediolateral (ML) axes (Figs. 2C, F). Injection of 5 ng of either of the morpholinos resulted in embryos exhibiting shorter AP axes than control embryos (Figs. 2E, H). As discussed in detail below, such gastrulation defects can result from a disruption of convergence and extension (C&E) movements. Embryos injected with 5 ng of either of the mismatch control morpholinos did not suffer from these defects (Figs. 2D, G). During somitogenesis, the somites of embryos injected with either of the morpholinos were compressed along the AP axis and wider along the ML axis (Figs. 2J, J′) as compared to the somites of uninjected embryos (data not shown) or control morpholino injected embryos (Figs. 2I–I′). At prim-5 stage and later on, embryos injected with either one of the morpholinos remained shorter than control siblings and showed broader and compressed somites (Figs. 2K, L). The severity of these defects increased in a dose-dependent manner, with a slightly higher penetrance observed for Lpp-MO/ATG compared to Lpp-MO/3e3i at equal dose (data not shown).

The identical phenotypes produced by the two non-overlapping morpholinos suggest that their effects are specific. To further examine the specificity of the observed defects after knockdown of *lpp*, rescue experiments were performed. These experiments, however, were difficult to interpret because overexpression of *lpp* often produced a phenotype similar to that observed following inhibition of *lpp* (data not shown). This phenomenon is not uncommon: a hallmark of the PCP genes is that their increased activity also impairs gastrulation (Adler and Lee, 2001; Darken et al., 2002; Heisenberg et al., 2000; Latinkic et al., 2003; Marlow et al., 2002; Sokol, 1996). Nevertheless, whereas only 22% of Lpp-MO/3e3i-injected embryos exhibited a normal phenotype, we observed that co-injection of 7.5 pg *lpp* mRNA increased this figure to 45% (Fig. 2M). Injection of 7.5 pg *lpp* mRNA alone resulted in about 19% of the embryos showing gastrulation defects, which may explain why we were not able to obtain a complete rescue. Taken together, our observations indicate that the effects of the Lpp-morpholinos are specific.

Knockdown of lpp expression disrupts C&E movements during gastrulation

Defective C&E movements after downregulation of Lpp were documented by whole-mount in situ hybridization analyzing the expression patterns of marker genes for the axial and paraxial mesoderm and neurectoderm in trunk and tail. At the onset of gastrulation the expression of *goosecoid* (*gsc*), which marks the presumptive dorsal mesoderm, appeared normal in morpholino injected embryos, indicating that *lpp* knockdown did not prevent mesoderm induction or differentiation (Fig. 3A). At the end of gastrulation, mild abnormalities in prechordal plate shape and position were observed, as assessed by *hatching gland 1* (*hgg1*) expression. The tissue appeared more elongated and was positioned slightly more posteriorly with respect to the anterior edge of the neural plate (Fig. 3B′). In contrast to these weak effects on the anterior axial mesoderm, we observed severe impairment of AP extension and ML convergence of more posterior axial mesoderm, leading to a shorter and broader notochord at tailbud stage, as indicated by the expression of *no tail* (*ntl*) (Fig. 3B). Therefore, it appeared that the most anterior axial mesoderm, as marked by *hgg1*, was less affected than the more posterior axial mesoderm, as marked

Fig. 2. Knockdown of *lpp* disrupts convergence and extension movements. (A, B) Validation of the morpholinos: (A) quantitative RT-PCR using total cDNA from tailbud stage embryos as a template, shows an 80% reduction of *lpp* expression after injection of Lpp-MO/3e3i but not after injection of Lpp-MM/3e3i; (B) Lpp protein levels of prim-5 stage embryos are strongly reduced after injection of Lpp-MO/ATG but not after injection of Lpp-MM/ATG, as shown by quantification of the intensities of the protein bands after Western blot analysis (cumulative results of three experiments). Error bars represent standard errors of the mean. (C–L) Morpholinos (Lpp-MO/ATG and Lpp-MO/3e3i) or mismatch control morpholinos (Lpp-MM/ATG and Lpp-MM/3e3i) were injected at the one- to two-cell stage and morphology was assessed at different stages. (C–H) tailbud stage, lateral view, dorsal to the right; the anterior-most structure is indicated with an arrow. (I, J) 5-somite stage, lateral view, dorsal to the right. (I′, J′) 5-somite stage, dorsal view; drawings schematically show the notochord and somites of the embryos in the pictures. (K, L) prim-5 stage, lateral view, anterior to the left. *Abbreviations*: NI, non-injected; ML, mediolateral axis; AP, anterior–posterior axis. (M) Zebrafish embryos were injected with Lpp-MO/3e3i (5 ng) or synthetic mRNA (7.5 pg) encoding full-length Lpp, or were co-injected with Lpp-MO/3e3i (5 ng) and synthetic *lpp* mRNA (7.5 pg). At tailbud stage, the embryos were scored morphologically for the presence of C&E defects, as depicted in panels E and H. The phenotypes of the embryos of three independent experiments were scored and the percentages of normal embryos, embryos with C&E defects ("CE defects") and embryos with defects other than C&E defects ("other defects") are indicated. *n*, total number of embryos injected for each condition.

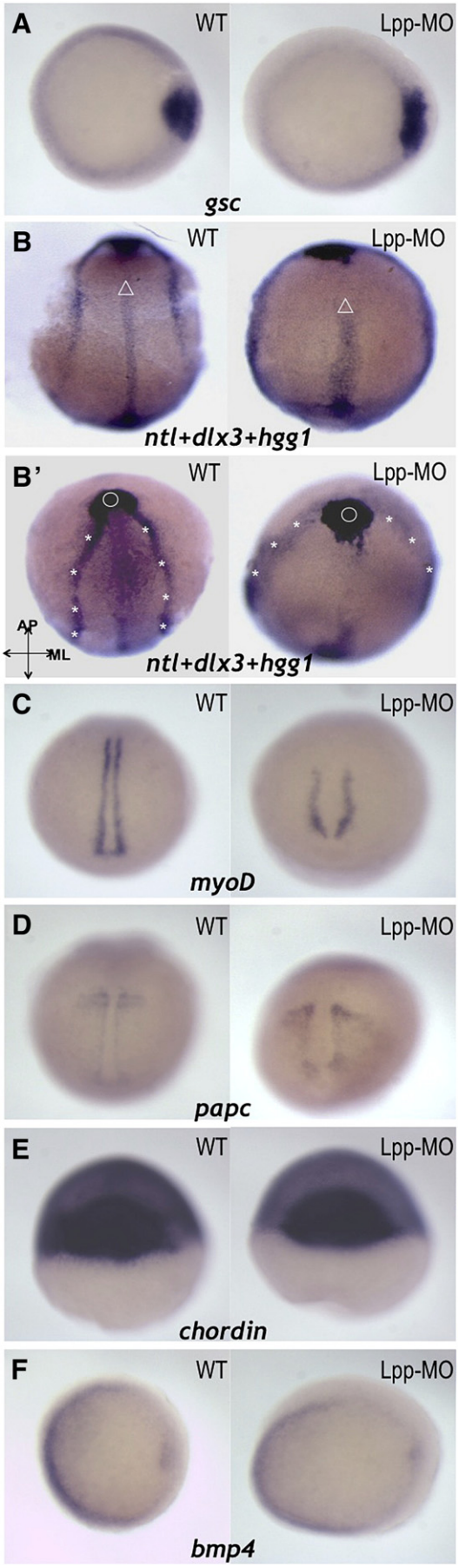

by *ntl*. *MyoD* expression in the paraxial mesoderm appeared to be anterior–posteriorly shortened and mediolaterally expanded at tailbud stage (Fig. 3C), and the similar broader and shorter posterior paraxial mesoderm was shown by *paraxial protocadherin* (*papc*) staining at the early somitogenesis stages (Fig. 3D). Also, in neurectoderm, the laterally expanded expression domain of *distal-less3* (*dlx3*) revealed a broader neural plate (Fig. 3B′). The expression pattern of the dorsal mesoderm marker *chordin* (Fig. 3E) as well as the ventral ectoderm marker *bone morphogenetic protein4* (*bmp4*) (Fig. 3F) were all unaffected, indicating that the lack of Lpp function does not interfere with dorso-ventral patterning and cell fate. All of these altered expression patterns indicate that C&E movements are impaired after knockdown of *lpp*, affecting both the axial and paraxial mesoderm and the neurectoderm.

Lpp is required for efficient dorsal convergence

To explore the cellular motility defect underlying the C&E phenotype after *lpp* knockdown, time-lapse analysis was performed. Paths of individual paraxial mesodermal cells were determined for wild-type (n=60 cells from 2 embryos) and Lpp-MO/ATG injected (n=60 cells from 2 embryos) embryos during the previously reported period of peak dorsal migration during mid to late gastrulation (Myers et al., 2002) (Figs. 4A, B). Analysis of total cell speeds (accounting for movement in all directions) revealed no significant difference between wild-type and Lpp-morphant cells (p=0.18) (Fig. 4E and Table S1). In contrast, the net dorsal speed of Lpp-morphant cells (accounting for dorsal movement) was reduced to only 50% of the wild-type net dorsal speed ($p=1.0\times10^{-8}$) (Fig. 4F and Table S1). Paraxial cells in wild-type embryos moved dorsally with little change in direction (Fig. 4C). In contrast, although the net paths of paraxial cells from Lpp-morphant embryos were dorsally directed, these cells appeared to change direction more frequently and consequently migrated toward the dorsal direction in a less effective way (Fig. 4D). These results indicate that impaired dorsal cell movement underlies the C&E defect after *lpp* knockdown.

Expression of lpp is dependent on Wnt/PCP signaling

The observed disruption of C&E after morpholino knockdown of Lpp function is strikingly similar to phenotypes reported for *silberblick/wnt11* loss-of-function zebrafish mutants disrupting PCP signaling (Heisenberg et al., 2000). Recently, it was shown in vitro in human iliac vein SMCs that *LPP* expression is dependent on RhoA/ROK signaling (Gorenne et al., 2006). RhoA and its effector Rho kinase 2 (Rok2) are downstream mediators of noncanonical Wnt11 in zebrafish (Marlow et al., 2002; Zhu et al., 2006). Together, these findings raise the possibility that Lpp acts downstream of Wnt11 and Rok2 to regulate C&E during zebrafish gastrulation.

To test whether *lpp* expression could be regulated by noncanonical Wnt11 signaling in zebrafish, we determined the amount of *lpp* mRNA after knockdown of Wnt11. Quantitative RT-PCR revealed a significant (p=0.021) reduction of *lpp* mRNA levels in zebrafish injected with Wnt11-MO, compared to *lpp* levels in wild-type controls (Fig. 5). A similar result was obtained after injection of RNA encoding a dominant-negative form of zebrafish Rok2 (dnRok2) (p=0.013) (Fig. 5). Significant reduction of *lpp* mRNA levels was also observed as a result of *wnt11* overexpression (p=0.006) (Fig. 5), consistent with observations that both gain and loss of morphogenetic Wnt11

Fig. 3. Expression of marker genes in *lpp* morphants. Wild-type embryos and embryos injected with Lpp-morpholino were analyzed for the expression domains of marker genes by whole mount in situ hybridization. In each section (A–F), wild-type (WT) embryos are depicted on the left and *lpp* morphants (Lpp-MO) on the right. (A) *gsc*, shield stage, animal pole view, dorsal to the right. (B, B′) *ntl* (Δ), *dlx-3* (*) and *hgg1* (O), tailbud stage, dorsal views (B) and animal pole views (B′) of the same embryo. (C) *myoD*, tailbud stage, dorsal view. (D) *papc*, two-somite stage, dorsal view. (E) *chordin*, shield stage, dorsal view. (F) *bmp4*, shield stage, animal pole view, dorsal to the right.

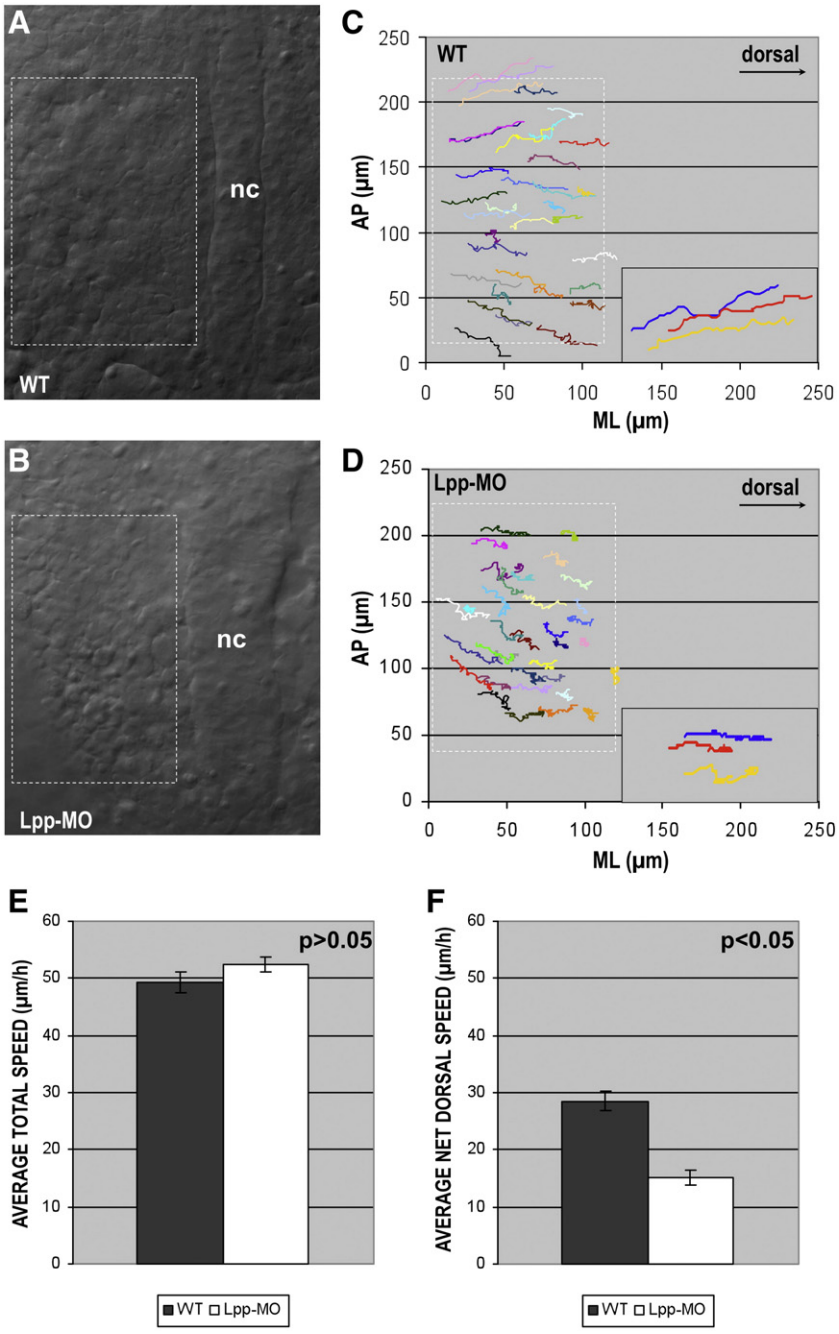

Fig. 4. Lpp function is required for efficient dorsal convergence. Dorsal views of (A) wild-type (WT) and (B) Lpp-MO/ATG (5 ng) injected embryos at tailbud stage (boxes highlight the paraxial region, which was the focus of the migration analysis). (C, D) Cell tracks of paraxial cells from (C) wild-type and (D) Lpp-MO/ATG injected embryos extracted from Normarski time-lapse images. Each graph shows representative data obtained from individual embryos. Insets are enlarged tracks of three representative cells. AP, anterior–posterior axis; ML, mediolateral axis. (E) No significant ($p=0.19$) difference in total speed (µm/h) could be detected between wild-type and Lpp-MO/ATG injected embryos, (F) whereas net dorsal speed after Lpp-MO/ATG injection was significantly ($p=1.1\times10^{-8}$) reduced. (E, F) Graphs represent average data from 60 cells from 2 embryos for each condition; error bars represent standard errors of the mean.

function impairs gastrulation (Tada and Smith, 2000). Furthermore, both *wnt11* and *rok2* mRNA levels remained unchanged after injection of Lpp-MO/ATG (5 ng) or Lpp-MM/ATG (5 ng), indicating that Lpp acts downstream of *wnt11* and *rok2* (data not shown). Together, these results support the idea that expression of *lpp* in zebrafish is, directly or indirectly, regulated by noncanonical Wnt/PCP signaling.

Lpp genetically interacts with scrib and trilobite during C&E movements

A genetic interaction was previously shown in mice between *Scrib* and the PCP gene *Vangl2* (Montcouquiol et al., 2003; Murdoch et al., 2003), implicating Scrib in the regulation of PCP. Recently, the genetic interaction between these genes was also established for their orthologues in zebrafish, *scrib* and *trilobite* respectively (Wada et al., 2005).

A direct interaction between the carboxy-terminus of human LPP and the PDZ domains of human SCRIB was shown previously (Petit et al., 2005b). Since theoretically, the C-terminus of zebrafish Lpp (-TDL) fulfils all known requirements for binding to Scrib-type PDZ domains, i.e. a hydrophobic amino acid at position 0 and a serine or threonine at position −2 (Hung and Sheng, 2002) (Fig. S1), we investigated whether this interaction also exists between Lpp and Scrib in zebrafish. To

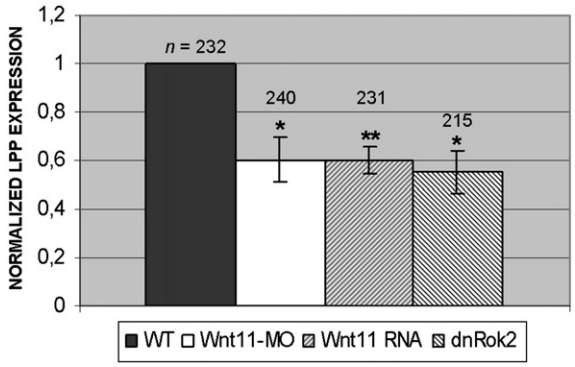

Fig. 5. *lpp* mRNA levels are reduced in Wnt11 morphants and in embryos overexpressing Wnt11 or a dominant negative form of Rho kinase 2. Zebrafish embryos were injected with Wnt11-MO (2 ng), *wnt11* RNA (100 pg) or *dnRok2* RNA (100 pg). Embryos showing clear C&E defects at tailbud stage were selected and total RNA was extracted. Quantitative RT-PCR with primers for *lpp* showed reduced levels of *lpp* mRNA in all three conditions (*, $p<0.05$; **, $p<0.01$). *n*, total number of embryos per condition from four independent experiments.

verify this experimentally, we performed GST pull-down analysis. An in vitro translated Scrib fragment containing all four PDZ domains (Scrib-PDZ_{WT}) was tested for binding to GST-Lpp-LT_{WT}, GST-Lpp-LT_{L557A} or GST alone. GST-Lpp-LT_{WT} contains 40 amino acids of the pre-LIM region, the three LIM domains and the wild-type carboxy-terminal tail of zebrafish Lpp. GST-Lpp-LT_{L557A} is identical to GST-Lpp-LT_{WT} except for a point mutation converting leucine^{557} (position 0) into alanine. All GST-fusion proteins, as well as GST alone could be robustly expressed in *E. coli* (Fig. 6A). As shown in Fig. 6B, Scrib-PDZ_{WT} interacted specifically with the wild-type Lpp protein but not with its mutated form or with GST alone. These results are consistent with a specific and direct interaction between Lpp and Scrib in zebrafish.

To assess whether Lpp and Scrib control C&E movements together, we performed genetic interaction experiments. Lpp-MO/ATG and a Scrib-morpholino (Scrib-MO) were titrated to suboptimal doses and co-injected to knockdown both proteins at the same time. As shown in Fig. 6C, separate injection of suboptimal doses of either morpholino led to no significant defects, compared to uninjected controls. However, injecting both morpholinos together resulted in C&E defects in about 50% of the injected embryos. The severity of these defects was comparable to those observed in embryos injected with optimal amounts (5 ng) of Lpp-MO/ATG or Scrib-MO that induce a phenotype in most (>90%) of the injected embryos. These results indicate that *lpp* and *scrib* genetically interact and, since they interact physically, that they act in the same pathway for the regulation of C&E.

Since *scrib* is known to genetically interact with *trilobite* in zebrafish (Wada et al., 2005), we also assessed whether there is a genetic interaction between *lpp* and *trilobite*. We co-injected suboptimal doses of the Lpp-MO/ATG and a morpholino against *trilobite* (Tri-MO) and counted the number of embryos showing clear C&E defects. Although the suboptimal dose of Tri-MO still resulted in mild defects of C&E movements, co-injection with the suboptimal dose of Lpp-MO/ATG caused severe C&E defects in more than 90% of the embryos (Fig. 6D).

Overall, these results indicate that *lpp*, *scrib* and *trilobite* genetically interact for the regulation of C&E during zebrafish gastrulation.

Discussion

Lpp function is required for convergence and extension movements during zebrafish gastrulation

During vertebrate gastrulation and neurulation, C&E reflects the medial migration and intercalation of mesodermal and neurectodermal cells. These movements are directed by lamellipodia on the medial and lateral faces of these cells and by the organized deposition of extracellular matrix fibrils (Keller et al., 2000; Wallingford et al., 2002), and lead to a significant elongation of the body axis. Such aligned cell behaviors require reorganization of the cytoskeleton and modulation of cell adhesion. Lpp, which localizes in focal adhesions and cell–cell contacts and interacts with cytoskeletal proteins such as α-actinin and VASP, is therefore a good candidate for being involved in these processes.

Our results indicate that Lpp plays a significant role in the regulation of C&E during zebrafish gastrulation. The temporal expression pattern of *lpp*, with highest expression in the early stages of zebrafish development, provides a first hint for its function during gastrulation. Moreover, we show that both morpholino-based knockdown and to a lesser degree overexpression led to a shortened body axis phenotype, a phenomenon also observed for other genes involved in gastrulation movements (Tada and Smith, 2000). Importantly, *lpp* morphants display embryonic defects similar to those when C&E is disrupted, such as reduced elongation of the body axis, broader and compressed somites and shorter and broader notochord, all of which are reminiscent of the phenotype of noncanonical Wnt signaling mutants (Heisenberg et al., 2000; Marlow et al., 2002; Sepich et al., 2000; Wada et al., 2005; Zhu et al., 2006). Time-lapse analysis showed that the total migration speed of paraxial cells was not significantly different between wild-type and Lpp-MO injected embryos. In contrast, net dorsal speed appeared to be strongly reduced after knockdown of *lpp* because of a failure of cells to move along straight paths. These results suggest that, during zebrafish gastrulation, Lpp is involved in cytoskeletal reorganization and subsequent mediolateral elongation, which controls the dorsal direction of migration rather than migration per se. Mediolateral elongation is also required for cells to intercalate at the dorsal midline. Although defective cell intercalation can be responsible for C&E defects as well, the observed reduced dorsal convergence before the cells reach the dorsal midline to intercalate, suggests that the first defect after knockdown of *lpp* is at the level of polarized migration. Lpp, being linked to cytoskeletal proteins such as VASP and α-actinin, is a good candidate for being involved in cytoskeletal reorganization. Likewise, an important role in the redistribution of the actin cytoskeleton was previously suggested for the interaction between VASP and zyxin (Drees et al., 2000; Rottner et al., 2001). Also, the interaction between Lpp and Scrib suggests that Lpp is involved in the regulation of cell polarity, which in turn is necessary for directional cell migration.

Expression of lpp is regulated by Wnt/PCP signaling

In *Xenopus* and zebrafish, a noncanonical Wnt signaling pathway constitutes the vertebrate PCP pathway and regulates mediolateral cell polarization underlying C&E (Keller et al., 1991; Warga and Kimmel, 1990). A known downstream effector of noncanonical Wnt11 in zebrafish is RhoA, a small GTPase of the Rho family (Zhu et al., 2006). Rho small GTPases play pivotal roles in cytoskeletal rearrangement, leading to a wide variety of cellular and developmental properties including changes in cell morphology and motility, cell adhesion, transcriptional regulation, differentiation and cell proliferation (Etienne-Manneville and Hall, 2002; Van Aelst and D'Souza-Schorey, 1997). A downstream effector of RhoA that partially mediates this action is the Rho-associated kinase (ROK). Two vertebrate isoforms of ROK have been identified: ROK1, which was first identified in human (Ishizaki et al., 1996), and ROK2, which was first identified in mice and is also known as ROKα (Leung et al., 1995) and Rho kinase (Matsui et al., 1996). In zebrafish, only the ROK2 isoform (Rok2) has been described so far (Riento and Ridley, 2003). The protein was found to act downstream of Wnt11 to mediate cell polarity and effective C&E movements in zebrafish (Marlow et al., 2002). Here, we show that knockdown or overexpression of Wnt11 results in a significant reduction of *lpp* mRNA levels, suggesting that *lpp* expression is at least partially regulated by noncanonical Wnt signaling in zebrafish.

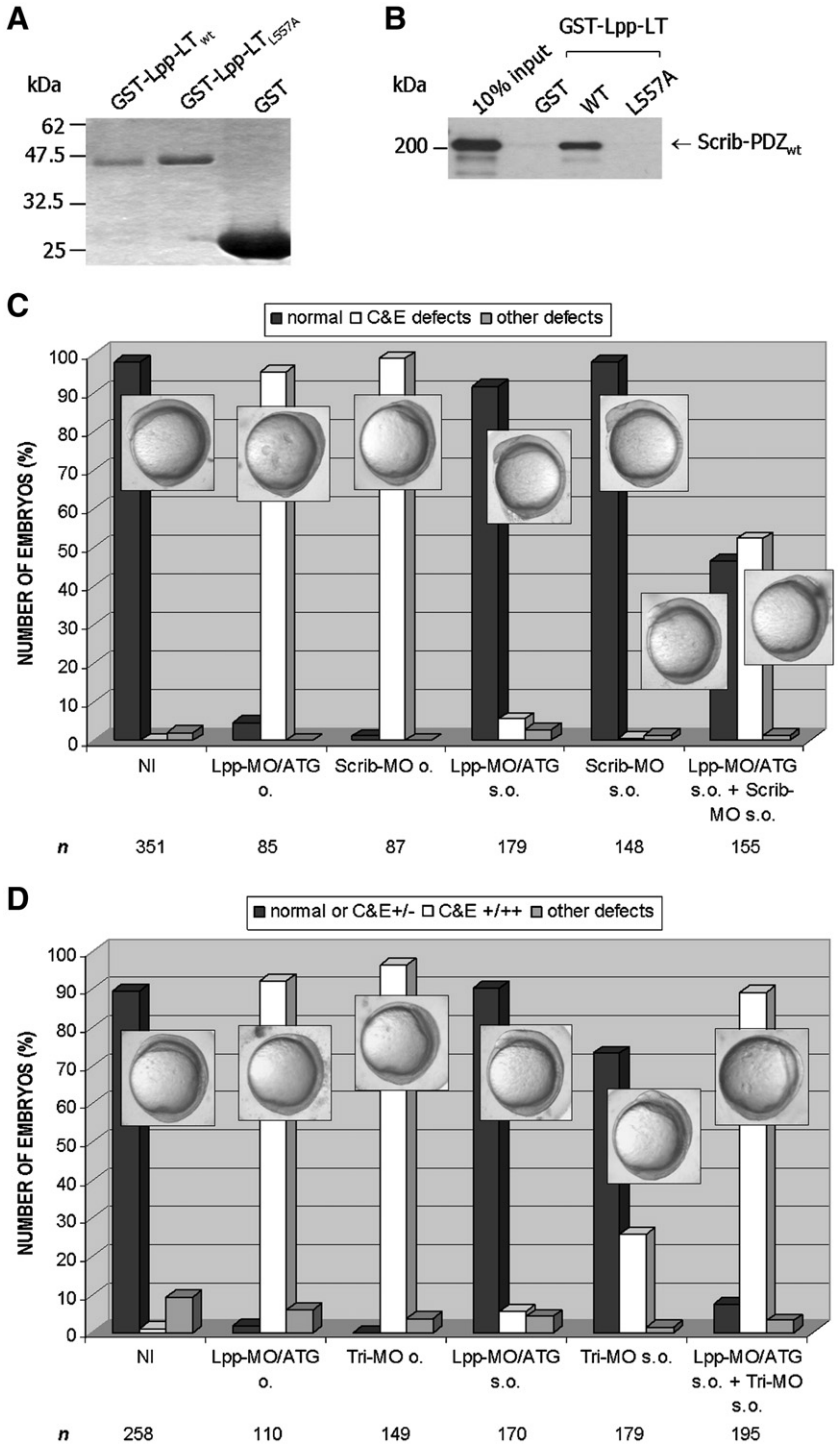

Fig. 6. *lpp* genetically interacts with *scrib* and *trilobite* for the regulation of C&E during zebrafish gastrulation. (A) GST fusion proteins, as indicated, and GST alone were expressed in *E. coli*, purified and analyzed by SDS-PAGE and GelCode Blue Stain Reagent staining. All proteins were expressed well. Protein markers are as indicated. (B) All four PDZ domains of wild-type zebrafish Scrib (AA 700–1517) were synthesized in vitro and ^{35}S-labeled. Labeled proteins were incubated with immobilized GST, GST-Lpp-LT$_{WT}$ or GST-Lpp-LT$_{L557A}$ and allowed to interact overnight at 4 °C. Bound proteins were eluted in sample buffer, separated by SDS-PAGE and visualized by autoradiography. The amount of synthesized protein loaded as a reference on the gel corresponds to 10% of the input used in each binding experiment. (C) Suboptimal doses (s.o.) of Lpp-MO/ATG (1 ng) or Scrib-MO (1 ng) were injected separately or were co-injected in the one- to two-cell stage; the phenotypes were scored at the five-somite stage and compared to embryos injected with optimal doses (o.) of either of the morpholinos (Lpp-MO, 5 ng; Scrib-MO, 5 ng). Phenotypes scored were: normal, C&E defects, and defects other than C&E defects ("other defects"). (D) Suboptimal doses (s.o.) of Lpp-MO/ATG (1 ng) or Tri-MO (0.25 ng) were injected separately or were co-injected in the one- to two-cell stage. The phenotypes were scored at 11 hpf and compared to embryos injected with optimal doses (o.) of either of the morpholinos (Lpp-MO, 5 ng; Tri-MO, 4 ng). Phenotypes scored were: normal or mild C&E defects (C&E+/−), moderate (C&E+) or strong (C&E++) C&E defects, and defects other than C&E defects ("other defects"). Pictures in panels C and D show for each condition embryos representative for the phenotype of the largest group(s). Abbreviations: NI, uninjected. *n*, total number of embryos per condition from two independent experiments.

Moreover, overexpression of dominant-negative *Rok2* also resulted in reduced *lpp* mRNA levels, indicating that Lpp acts downstream of RhoA/Rok2. In this regard it is interesting to mention that in vitro experiments in human derived SMCs also show that LPP expression is RhoA/ROK dependent (Gorenne et al., 2006), suggesting that RhoA/ROK regulation of LPP expression is conserved among vertebrates. The

observation that *lpp* mRNA levels are reduced after both knockdown and overexpression of *wnt11* is in agreement with previous reports that knockdown as well as overexpression of *wnt11* in zebrafish results in C&E defects (Heisenberg et al., 2000). These results are also consistent with an in vivo experiment in zebrafish embryos, in which overexpression of *wnt11* results in cytoplasmic localization and, therefore, inactivation of Rok2 (Marlow et al., 2002).

Lpp cooperates with PCP genes scrib and trilobite to mediate convergence and extension movements during zebrafish gastrulation

Scrib is a member of the LAP (leucine-rich repeat and PDZ) family of proteins that is involved in the regulation of cell adhesion, cell shape and cell polarity (Bilder and Perrimon, 2000). *Scrib* was previously identified as a PCP gene in mice through its genetic interaction with *Vangl2*. Recently, this genetic interaction was also established in zebrafish, and it was shown that maternal expression of Scrib is required for C&E movements during gastrulation (Wada et al., 2005). One proposed explanation for this interaction is that the observed apical localization of all core PCP proteins is dependent on Scribble-based apical/basal cell polarity (Karner et al., 2006).

In humans, a direct interaction between LPP and SCRIB was shown previously (Petit et al., 2005a), but so far, no studies have been performed to address the possible functionality of this interaction. We have now shown that Lpp and Scrib physically interact in zebrafish as well, and moreover, we show that they interact genetically for the regulation of C&E. As such, for the first time, we provide evidence for a developmental role of the Lpp–Scrib interaction. The genetic interaction observed between *lpp* and *trilobite*, is likely to be a consequence of the Lpp–Scrib interaction.

Conclusion: Lpp plays a crucial role during early zebrafish embryogenesis

Human LPP localizes to cell adhesion sites where it interacts with α-actinin, VASP and Scrib. It is therefore likely to play a role in mediating events such as cytoskeletal reorganization and modulation of cell adhesion, processes that could ultimately lead to mediolateral elongation and polarized cell migration. All of these binding sites are conserved in zebrafish Lpp, providing a possible mechanism through which downregulation of *lpp* expression could account for the observed C&E defects.

The results described in this paper indicate that expression of *lpp* in zebrafish is dependent on noncanonical Wnt/PCP signaling and that it plays a crucial role during early zebrafish embryogenesis in the regulation of C&E. More specifically, we demonstrate that knockdown of *lpp* leads to a reduced ability of cells to move in an oriented manner, leading to reduced dorsal convergence and consequently C&E defects. In addition, we show that Lpp and the PCP protein Scrib interact genetically as well as physically and, as such, that they act in the same pathway for the regulation of C&E during zebrafish gastrulation.

Acknowledgments

We thank Bart De Cat for helpful comments and discussions throughout the course of this work, and Guido David for a critical reading of the manuscript. We also thank Nathalie Delande and Rob Deckers for excellent technical assistance and Steffen Fieuws (Biostatistical Center, University Hospital Leuven, Belgium) for statistical advice. This work was supported in part by the "Geconcerteerde Onderzoeksactie" (GOA-010, 2002–2006 and GOA/2006/13), the Fund for Scientific Research—Flanders (Grant G.0290.7), the "Fortis Bank (FB) Verzekeringen-programma voor Kankeronderzoek" and the Foundation for Biochemical and Pharmaceutical Research and Education. This research was also achieved thanks to a scientific research fund of the Belgian Federation against Cancer, a non profit organization. Marleen Petit is a recipient of a "postdoctoraal beleidsmandaat van het Bijzonder Onderzoeksfonds (BOF) K.U.Leuven" (PDM/06/253/BM).

Appendix A. Supplementary data

Supplementary data associated with this article can be found, in the online version, at doi:10.1016/j.ydbio.2008.05.529.

References

Adler, P.N., Lee, H., 2001. Frizzled signaling and cell–cell interactions in planar polarity. Curr. Opin. Cell Biol. 13, 635–640.
Akimenko, M.A., Ekker, M., Wegner, J., Lin, W., Westerfield, M., 1994. Combinatorial expression of three zebrafish genes related to distal-less: part of a homeobox gene code for the head. J. Neurosci. 14, 3475–3486.
Bilder, D., Perrimon, N., 2000. Localization of apical epithelial determinants by the basolateral PDZ protein Scribble. Nature 403, 676–680.
Daheron, L., Veinstein, A., Brizard, F., Drabkin, H., Lacotte, L., Guilhot, F., Larsen, C.J., Brizard, A., Roche, J., 2001. Human LPP gene is fused to MLL in a secondary acute leukemia with a *t*(3;11) (q28;q23). Genes Chromosomes Cancer 31, 382–389.
Dahlen, A., Mertens, F., Rydholm, A., Brosjo, O., Wejde, J., Mandahl, N., Panagopoulos, I., 2003. Fusion, disruption, and expression of HMGA2 in bone and soft tissue chondromas. Mod. Path. 16, 1132–1140.
Darken, R.S., Scola, A.M., Rakeman, A.S., Das, G., Mlodzik, M., Wilson, P.A., 2002. The planar polarity gene strabismus regulates convergent extension movements in *Xenopus*. EMBO J. 21, 976–985.
Drees, B., Friederich, E., Fradelizi, J., Louvard, D., Beckerle, M.C., Golsteyn, R.M., 2000. Characterization of the interaction between zyxin and members of the Ena/vasodilator-stimulated phosphoprotein family of proteins. J. Biol. Chem. 275, 22503–22511.
Etienne-Manneville, S., Hall, A., 2002. Rho GTPases in cell biology. Nature 420, 629–635.
Gorenne, I., Nakamoto, R.K., Phelps, C.P., Beckerle, M.C., Somlyo, A.V., Somlyo, A.P., 2003. LPP, a LIM protein highly expressed in smooth muscle. Am. J. Physiol., Cell Physiol. 285, C674–685.
Gorenne, I., Jin, L., Yoshida, T., Sanders, J.M., Sarembock, I.J., Owens, G.K., Somlyo, A.P., Somlyo, A.V., 2006. LPP expression during in vitro smooth muscle differentiation and stent-induced vascular injury. Circ. Res. 98, 378–385.
Guo, B., Sallis, R.E., Greenall, A., Petit, M.M., Jansen, E., Young, L., Van de Ven, W.J., Sharrocks, A.D., 2006. The LIM domain protein LPP is a coactivator for the ETS domain transcription factor PEA3. Mol. Cell. Biol. 26, 4529–4538.
Heisenberg, C.P., Tada, M., Rauch, G.J., Saude, L., Concha, M.L., Geisler, R., Stemple, D.L., Smith, J.C., Wilson, S.W., 2000. Silberblick/Wnt11 mediates convergent extension movements during zebrafish gastrulation. Nature 405, 76–81.
Hung, A.Y., Sheng, M., 2002. PDZ domains: structural modules for protein complex assembly. J. Biol. Chem. 277, 5699–5702.
Ishizaki, T., Maekawa, M., Fujisawa, K., Okawa, K., Iwamatsu, A., Fujita, A., Watanabe, N., Saito, Y., Kakizuka, A., Morii, N., Narumiya, S., 1996. The small GTP-binding protein Rho binds to and activates a 160 kDa Ser/Thr protein kinase homologous to myotonic dystrophy kinase. EMBO J. 15, 1885–1893.
Jin, L., Kern, M.J., Otey, C.A., Wamhoff, B.R., Somlyo, A.V., 2007. Angiotensin II, focal adhesion kinase, and PRX1 enhance smooth muscle expression of lipoma preferred partner and a newly identified lipoma preferred partner binding partner palladin to promote cell migration. Circ. Res. 100, 817–825.
Karner, C., Wharton Jr., K.A., Carroll, T.J., 2006. Planar cell polarity and vertebrate organogenesis. Semin. Cell Dev. Biol. 17, 194–203.
Keller, R., Clark, W.H.J., Griffin, F., 1991. Gastrulation. Movements, patterns, and molecules. Plenum Press, New York.
Keller, R., Davidson, L., Edlund, A., Elul, T., Ezin, M., Shook, D., Skoglund, P., 2000. Mechanisms of convergence and extension by cell intercalation. Philos. Trans. R. Soc. Lond., B Biol. Sci. 355, 897–922.
Kimmel, C.B., Ballard, W.W., Kimmel, S.R., Ullmann, B., Schilling, T.F., 1995. Stages of embryonic development of the zebrafish. Dev. Dyn. 203, 253–310.
Krieg, P.A., Melton, D.A., 1984. Functional messenger RNAs are produced by SP6 in vitro transcription of cloned cDNAs. Nucleic Acids Res. 12, 7057–7070.
Latinkic, B.V., Mercurio, S., Bennett, B., Hirst, E.M., Xu, Q., Lau, L.F., Mohun, T.J., Smith, J.C., 2003. Xenopus Cyr61 regulates gastrulation movements and modulates Wnt signalling. Development 130, 2429–2441.
Leung, T., Manser, E., Tan, L., Lim, L., 1995. A novel serine/threonine kinase binding the Ras-related RhoA GTPase which translocates the kinase to peripheral membranes. J. Biol. Chem. 270, 29051–29054.
Li, B., Zhuang, L., Reinhard, M., Trueb, B., 2003. The lipoma preferred partner LPP interacts with alpha-actinin. J. Cell Sci. 116, 1359–1366.
Livet, J., Sigrist, M., Stroebel, S., De Paola, V., Price, S.R., Henderson, C.E., Jessell, T.M., Arber, S., 2002. ETS gene Pea3 controls the central position and terminal arborization of specific motor neuron pools. Neuron 35, 877–892.
Marlow, F., Topczewski, J., Sepich, D., Solnica-Krezel, L., 2002. Zebrafish Rho kinase 2 acts downstream of Wnt11 to mediate cell polarity and effective convergence and extension movements. Curr. Biol. 12, 876–884.
Matsui, T., Amano, M., Yamamoto, T., Chihara, K., Nakafuku, M., Ito, M., Nakano, T., Okawa, K., Iwamatsu, A., Kaibuchi, K., 1996. Rho-associated kinase, a novel serine/threonine kinase, as a putative target for small GTP binding protein Rho. EMBO J. 15, 2208–2216.

Montcouquiol, M., Rachel, R.A., Lanford, P.J., Copeland, N.G., Jenkins, N.A., Kelley, M.W., 2003. Identification of Vangl2 and Scrb1 as planar polarity genes in mammals. Nature 423, 173–177.

Murdoch, J.N., Henderson, D.J., Doudney, K., Gaston-Massuet, C., Phillips, H.M., Paternotte, C., Arkell, R., Stanier, P., Copp, A.J., 2003. Disruption of scribble (Scrb1) causes severe neural tube defects in the circletail mouse. Hum. Mol. Genet. 12, 87–98.

Myers, D.C., Sepich, D.S., Solnica-Krezel, L., 2002. Bmp activity gradient regulates convergent extension during zebrafish gastrulation. Dev. Biol. 243, 81–98.

Nelander, S., Mostad, P., Lindahl, P., 2003. Prediction of cell type-specific gene modules: identification and initial characterization of a core set of smooth muscle-specific genes. Genome Res. 13, 1838–1854.

Park, M., Moon, R.T., 2002. The planar cell-polarity gene stbm regulates cell behaviour and cell fate in vertebrate embryos. Nat. Cell Biol. 4, 20–25.

Petit, M.M., Mols, R., Schoenmakers, E.F., Mandahl, N., Van de Ven, W.J., 1996. LPP, the preferred fusion partner gene of HMGIC in lipomas, is a novel member of the LIM protein gene family. Genomics 36, 118–129.

Petit, M.M., Swarts, S., Bridge, J.A., Van de Ven, W.J., 1998. Expression of reciprocal fusion transcripts of the HMGIC and LPP genes in parosteal lipoma. Cancer Genet. Cytogenet. 106, 18–23.

Petit, M.M., Fradelizi, J., Golsteyn, R.M., Ayoubi, T.A., Menichi, B., Louvard, D., Van de Ven, W.J., Friederich, E., 2000. LPP, an actin cytoskeleton protein related to zyxin, harbors a nuclear export signal and transcriptional activation capacity. Mol. Biol. Cell 11, 117–129.

Petit, M.M., Meulemans, S.M., Van de Ven, W.J., 2003. The focal adhesion and nuclear targeting capacity of the LIM-containing lipoma-preferred partner (LPP) protein. J. Biol. Chem. 278, 2157–2168.

Petit, M.M., Crombez, K.R., Vervenne, H.B., Weyns, N., Van de Ven, W.J., 2005a. The tumor suppressor Scrib selectively interacts with specific members of the zyxin family of proteins. FEBS Lett. 579, 5061–5068.

Petit, M.M., Meulemans, S.M., Alen, P., Ayoubi, T.A., Jansen, E., Van de Ven, W.J., 2005b. The tumor suppressor Scrib interacts with the zyxin-related protein LPP, which shuttles between cell adhesion sites and the nucleus. BMC Cell Biol. 6, 1.

Riento, K., Ridley, A.J., 2003. Rocks: multifunctional kinases in cell behaviour. Nat. Rev., Mol. Cell Biol. 4, 446–456.

Rogalla, P., Lemke, I., Kazmierczak, B., Bullerdiek, J., 2000. An identical HMGIC-LPP fusion transcript is consistently expressed in pulmonary chondroid hamartomas with *t*(3;12)(q27–28;q14–15). Genes Chromosomes Cancer 29, 363–366.

Rottner, K., Krause, M., Gimona, M., Small, J.V., Wehland, J., 2001. Zyxin is not colocalized with vasodilator-stimulated phosphoprotein (VASP) at lamellipodial tips and exhibits different dynamics to vinculin, paxillin, and VASP in focal adhesions. Mol. Biol. Cell 12, 3103–3113.

Schulte-Merker, S., Ho, R.K., Herrmann, B.G., Nusslein-Volhard, C., 1992. The protein product of the zebrafish homologue of the mouse T gene is expressed in nuclei of the germ ring and the notochord of the early embryo. Development 116, 1021–1032.

Sepich, D.S., Myers, D.C., Short, R., Topczewski, J., Marlow, F., Solnica-Krezel, L., 2000. Role of the zebrafish trilobite locus in gastrulation movements of convergence and extension. Genesis 27, 159–173.

Shepherd, T.G., Kockeritz, L., Szrajber, M.R., Muller, W.J., Hassell, J.A., 2001. The pea3 subfamily ets genes are required for HER2/Neu-mediated mammary oncogenesis. Curr. Biol. 11, 1739–1748.

Sokol, S.Y., 1996. Analysis of Dishevelled signalling pathways during *Xenopus* development. Curr. Biol. 6, 1456–1467.

Tada, M., Smith, J.C., 2000. Xwnt11 is a target of *Xenopus brachyury*: regulation of gastrulation movements via Dishevelled, but not through the canonical Wnt pathway. Development 127, 2227–2238.

Thisse, C., Thisse, B., 1998. High resolution whole-mount in situ hybridization. Zebrafish Sci. Mon. 5, 8–9.

Thisse, C., Thisse, B., Halpern, M.E., Postlethwait, J.H., 1994. Goosecoid expression in neurectoderm and mesendoderm is disrupted in zebrafish cyclops gastrulas. Dev. Biol. 164, 420–429.

Ulrich, F., Krieg, M., Schotz, E.M., Link, V., Castanon, I., Schnabel, V., Taubenberger, A., Mueller, D., Puech, P.H., Heisenberg, C.P., 2005. Wnt11 functions in gastrulation by controlling cell cohesion through Rab5c and E-cadherin. Dev. Cell 9, 555–564.

Van Aelst, L., D'Souza-Schorey, C., 1997. Rho GTPases and signaling networks. Genes Dev. 11, 2295–2322.

Van Raay, T.J., Coffey, R.J., Solnica-Krezel, L., 2007. Zebrafish Naked1 and Naked2 antagonize both canonical and non-canonical Wnt signaling. Dev. Biol. 309, 151–168.

Wada, H., Iwasaki, M., Sato, T., Masai, I., Nishiwaki, Y., Tanaka, H., Sato, A., Nojima, Y., Okamoto, H., 2005. Dual roles of zygotic and maternal Scribble1 in neural migration and convergent extension movements in zebrafish embryos. Development 132, 2273–2285.

Wallingford, J.B., Fraser, S.E., Harland, R.M., 2002. Convergent extension: the molecular control of polarized cell movement during embryonic development. Dev. Cell 2, 695–706.

Wang, Y., Nathans, J., 2007. Tissue/planar cell polarity in vertebrates: new insights and new questions. Development 134, 647–658.

Warga, R.M., Kimmel, C.B., 1990. Cell movements during epiboly and gastrulation in zebrafish. Development 108, 569–580.

Westerfield, M., 1995. The zebrafish book. Univ of Oregon Press, Eugene, OR.

Zhu, S., Liu, L., Korzh, V., Gong, Z., Low, B.C., 2006. RhoA acts downstream of Wnt5 and Wnt11 to regulate convergence and extension movements by involving effectors Rho kinase and Diaphanous: use of zebrafish as an in vivo model for GTPase signaling. Cell. Signal. 18, 359–372.